ANTICANCER RESEARCH *33*: 1525-1536 (2013)

Normal Mammary Fibroblasts Induce Reversion of the Malignant Phenotype in Human Primary Breast Cancer

ANNA-MARIA RÖMER[1], INKE LÜHR[1], ANDREAS KLEIN[2], ANDREAS FRIEDL[3], SUSANNE SEBENS[4], FRANK RÖSEL[1], NORBERT ARNOLD[1], ALEXANDER STRAUSS[1], WALTER JONAT[1] and MARET BAUER[1]

[1]*Department of Gynecology and Obstetrics, University Medical Center Schleswig-Holstein, Kiel, Germany;*
[2]*Institute of Biochemistry, Charité, Virchow Campus Clinic, Berlin, Germany;*
[3]*Department of Pathology and Laboratory Medicine, University of Wisconsin-Madison, Madison, WI, USA;*
[4]*Institute of Experimental Medicine, Christian Albrechts University, Kiel, Germany*

Abstract. *Background/Aim: The tumor microenvironment plays a major role in tumor growth and progression. Its manipulation can lead to a reversion of the malignant phenotype. Here we explored the ability of normal mammary fibroblasts (HMFs) to induce reversion of the malignant phenotype of primary breast carcinoma cells (PBCs) in a three-dimensional (3D) context. Materials and Methods: PBCs were isolated from 13 primary breast carcinomas and cultured in 3D collagen-I gels as mono- or co-culture with HMFs. Results: In five co-cultures, PBCs exhibited reversion of their malignant phenotype, whereas PBCs in matched monocultures exhibited disorganized growth. Reversion, defined as the restoration of the complete baso-apical polarity axis, was confirmed with established polarity markers. Secretion of the tissue-specific glycoprotein MAM-6 into the acinar lumens and deposition of basement membrane indicated functional differentiation. Gene expression analysis revealed a set of differentially regulated genes which possibly affect the reversion process. These included MAL, ELF5, MAP6, ZMYND11 and SQLE. Conclusion: These findings highlight the significant role of fibroblasts in regulating the carcinoma phenotype.*

The mammary gland consists of various cell types that interact in a complex network that is required for proper development. A bi-layered epithelium is composed of luminal secretory cells and basal myoepithelial cells lines, ducts and acini. The myoepithelial cells produce the basement membrane (BM) as barrier between the epithelial and stromal compartment (1). Milk ducts and acini are surrounded by the stroma comprising of a variety of different cell types including adipocytes, fibroblasts, endothelial cells, immune cells and the extracellular matrix (ECM) (2). The epithelium and its surrounding microenvironment should be viewed as the functional unit of the mammary gland (3). Abundant evidence indicates that interactions between the epithelium and the microenvironment modulate epithelial differentiation and polarity, as well as proliferation, survival, migration and invasion (1).

The mammary epithelium can also undergo malignant transformation, proliferate and eventually become invasive. However, the mammary stroma contributes to both tumor promoting and permissive signals (4, 5). It is well-established that dramatic changes occur in the surrounding stroma during breast cancer development. The tumor microenvironment is characterized by an increased number of fibroblasts expressing alpha-smooth muscle actin, so-called cancer-associated fibroblasts (CAF), and fibrosis, collectively referred to as desmoplasia (6). The tumor microenvironment is one of the main regulators of tumor growth and invasiveness which can also provide protection from the human immune system attacking the cancer cells (3, 7, 8).

Experimental evidence from a variety of investigators has demonstrated that it is possible to restore a normal epithelial phenotype in carcinoma cells by adjusting their microenvironment (9, 10). Furthermore, it was shown that epigenetic changes take place throughout the reversion process (11). Remarkably, these findings demonstrate that malignant behavior is reversible when invasive breast cancer cells are placed in a defined microenvironment and that chromatin organization and adjustments to the intracellular signaling milieu can dominate a mutated genome (12-14). Nevertheless, the underlying mechanism of this reversion process remains incompletely understood.

The aim of this study was to investigate the influence of normal human mammary fibroblasts (HMFs) on the growth

Correspondence to: Maret Bauer, Department of Gynecology and Obstetrics, University Medical Center Schleswig-Holstein, Arnold-Heller-Str. 3, 24105 Kiel, Germany. E-mail: maret_bauer@yahoo.de

Key Words: Breast cancer, phenotypic reversion, microenvironment, mammary fibroblasts, primary cells.

and morphology of primary breast cancer cells (PBCs) and to assess their ability to induce reversion of the malignant phenotype of a pre-determined tumorigenic epithelium in a 3D cell culture model. By using HMFs in co-culture with PBCs we confronted the cancer cells with a normalized, non-malignant stroma. This approach disables the adverse interactions between the altered tumor microenvironment and the cancer cells and places the PBCs in a context that mimicks normal mammary gland. Additionally, we sought to compare, at the molecular level, carcinomas that could be reverted with those that showed no signs of reversion in our experiments.

Materials and Methods

Tissue samples and cell isolation. Tissues were obtained in compliance with the Helsinki Declaration with informed consent approved by the Institutional Review Board of the University Medical Center Schleswig-Holstein, Campus Kiel, Germany. PBCs were isolated from fresh surgical specimen from 13 patients with primary invasive breast carcinoma. The obtained tissue was minced into small pieces and digested in Dulbecco's Modified Eagle's Medium (DMEM, Life Technologies GmbH, Darmstadt, Germany) containing 2 mg/ml collagenase-I (BD Biosciences, Heidelberg, Germany) and 2 mg/ml hyaluronidase (SIGMA-ALDRICH Chemie GmbH, Steinheim, Germany) at 37˚C, with constant agitation for 2 h. Cells were centrifuged, pellets were washed with 10 ml Hank's Balanced Salt Solution (HBSS, Life Technologies GmbH) and centrifuged again. Cells were resuspended in trypsin/EDTA (0.25%) (SIGMA-ALDRICH Chemie GmbH) and incubated at 37˚C for 10 min with constant agitation. Cells were diluted with ice-cold DMEM (Life Technologies GmbH) and filtered through 100 μm and 40 μm cell strainers (BD Biosciences, Bedford, MA USA). The flow-through was centrifuged and the pellet containing the PBCs was resuspended and grown in H14-medium (15). Contamination of primary cultures with fibroblasts was removed using differential trypsinization (16). The purity of the PBC cultures was confirmed by immunolabeling for the epithelial cell marker pancytokeratin (polyclonal rabbit, 1:100; Abcam, Berlin, Germany) and the mesenchymal marker vimentin (monoclonal mouse, 1:100, Labvision/Thermo Fisher Scientific, Kalamazoo, MI, USA).

3-Dimensional cell culture. Normal human mammary fibroblasts (HMFs) (17) labeled with green fluorescent protein were used in co-cultures and cultured as described previously (15).

PBCs were cultured in 3D collagen-I gels both as mono- and as co-culture with HMFs. 3D cultures were prepared and maintained as described previously (15), with the following modifications: In monocultures, $0.05*10^6$ PBC/ml were used and in co-cultures, PBCs and HMFs were used at a ratio of 1:2 ($0.05*10^6$ PBC/ml and $0.1*10^6$ HMFs/ml).

Immunofluorescence analysis and image acquisition. For the quantification of cell growth and morphology assessment, collagen gels were fixed and stained as described previously (18). For immunostaining the following primary antibodies were used: monoclonal mouse anti-golgin-97 (1:100; Life Technologies GmbH), monoclonal mouse anti-β4-integrin (1:300; BD Biosciences, Heidelberg, Germany), monoclonal mouse anti-β1-integrin (1:200; Labvision/Thermo Fisher), polyclonal rabbit anti-β-catenin (1:100; Labvision/Thermo Fisher), monoclonal mouse anti-carcinoma-associated antigen (MAM-6; 1:50; Hycult Biotechnology, Uden, The Netherlands), polyclonal rabbit anti-ZO-I (1:25; New England Biolabs GmbH, Ipswich, MA, USA) and polyclonal rabbit anti-laminin-111 (1:1000; Abcam). Secondary antibodies were used as described previously (15). Immunostaining and immunofluorescent image acquisition was performed according to Lühr *et al*. (15) with modifications: For quantification of cell growth, 12 visual fields of each sample were analyzed. Cell morphology in co-culture was compared to that in monoculture to determine reversion of the malignant phenotype. Reversion was defined as the formation of polarized acini composed of a single layer of PBCs surrounding a hollow lumen. Polarity was identified by expression of golgin-97 at the apical cell pole and by basally-localized β4-integrin. Disorganized cell clusters were defined as apolar aggregates with irregular shape (length >2-fold width) without lumen formation. Cell aggregates were enumerated and classified according to their morphology. 3D Cultures with a significant difference in the number of polarized acini in co-culture compared to monoculture were defined as reversed. A minimum of 10 visual fields containing at least 60 cell clusters were evaluated for each sample.

Microarray analysis. Gene expression profiles of the original tumors used for five revertible and five non-revertible cell cultures were analyzed using the Affymetrix HG-U133 Plus 2.0 GeneChip. Those for the five non-reversible cell cultures were randomly chosen out of the collective of non-reversible breast cancer samples. RNA of breast carcinoma cells from the fresh frozen surgical specimen was extracted using the RNeasy Micro kit, according to the manufacturer's instructions (Qiagen, Hilden, Germany) and quantity and quality of the RNA samples were determined using the Agilent RNA 6000 Nano kit (Agilent Technologies, Waldbronn, Germany). cRNA was amplified from 3 μg of total RNA using the MessageAmp™ II-Biotin Enhanced Single Round cRNA Amplification Kit (Applied Biosystems, Darmstadt, Germany). Human genome HG-U133 Plus 2.0 GeneChip arrays were then hybridized with the biotin-labeled cRNA fragments for 16 h at 45˚C. Washing steps for the chip, staining with streptavidin-phycoerythrin, signal-amplification and scanning were performed according to the manufacturer's instructions (Affymetrix, Santa Clara, CA, USA).

Semi-quantitative real-time polymerase chain reaction (PCR). For validation of the results obtained by the microarray analysis, seven genes were chosen for RT-PCR based on their expression levels found in the microarray analysis and on biologically relevant information given in recent literature. Levels of three up-regulated E74-like factor-5 (ets domain transcription factor, ELF5), Mucin-like 1 (*MUCL1*), Prolactin-induced protein (*PIP*) and four down-regulated Microtubule-associated protein-6 (*MAP6*), Zinc finger, MYND-domain containing 11 (*ZMYND11*), Leucine-rich repeat and Ig domain containing-1 (*LINGO1*), Squalene epoxidase (*SQLE*) genes were determinated by qRT-PCR. cDNA was prepared from 1 μg RNA extracted from the tumors as described before using the QuantiTect Rev. Transcription Kit (Qiagen) according to the manufacturer's instructions. Primers were used at 20 μmol/μl stock concentration (all

Table I. *Patients' characteristics. Tissues for cell isolation were obtained from thirteen patients with primary invasive breast cancer without prior treatment.*

Patient ID	Age (years)	Histological subtype	Tumor stage (T)	Lymph nodes status (N)	Grade	ER*	PR*	HER2 status	Phenotypic reversion
1	81	Invasive ductal	pT4b	x	G3	12	2	Negative	+
2	84	Ductulo-lobular	pT4b	x	G2	12	6	Negative	+
3	71	Invasive ductal	pT1c	pN0 (0/4)	G3	6	0	Positive	+
4	84	Invasive ductal	pT1b	pN0 (0/2)	G1	12	12	Negative	+
5	45	Invasive ductal	pT1c	pN0 (0/24)	G3	8	4	Negative	+
6	63	Invasive ductal	pT2	pN1mic (1/18)	G2	12	12	Negative	–
7	45	Invasive ductal	pT1b	pN1a (1/24)	G3	0	0	Negative	–
8	71	Invasive ductal	pT4b	pN2a (8/10)	G2	12	9	Negative	–
9	61	Invasive lobular	pT2	pN0 (0/5)	G2	12	8	Negative	–
10	72	Neuroendocrine	pT3	pN0 (0/7)	G2	12	12	Negative	–
11	73	Invasive lobular	pT3	pN2a (8/17)	G2	12	6	Negative	–
12	43	Invasive ductal	pT1c	pN0 (0/4)	G3	8	6	Negative	–
13	48	Invasive ductal	pT3	pN3a (12/12)	G1	12	12	Negative	–

x, No information available; ER, estrogen receptor; PR, progesterone receptor; HER2, human epidermal growth factor receptor-2; +, phenotypic reversion; – no phenotypic reversion. *Expression of ER and PR was assessed using the immunoreactive score of Remmele and Stegner (27).

Qiagen; reference # *PIP*: QT01006026; *ELF5*: QT00004046; *MUCL1*: QT00051065; *ZMYND11*: QT00030961; *SQLE*: QT00012243; *MAP6*: QT00034524; *LINGO1*: QT01027950). Quantification of mRNA was carried out using the SYBR Green method on an iCycler iQ™ Real-Time PCR Detection System (both Bio-Rad Laboratories, Inc., Hercules, CA, USA). PCR mix (25 μl) was used for the real-time PCR assay that consisted of 12.5 μl SYBR Green Super Mix (Bio-Rad Laboratories), 2.5 μl primer from each stock, 8 μl of water or 4 μl and 4 μl of MgCl2, and 2 μl of template. PCR for *PIP*, *LINGO1*, *ZMYND11* and *MAP6* were carried out without $MgCl_2$, and that for *MUCL1*, *SQLE* and *ELF5* were carried out with $MgCl_2$. The thermal conditions consisted of an initial denaturation at 95˚C for 3 min, followed by 40 repeats of 95˚C for 30 sec, 64˚C for 7 sec and 72˚C for 7 sec. Then PCR was run for 1 min at 95˚C and 1 min at 64˚C followed by a cycle of 62-times 10 sec at 64˚C with an increase of set point temperature after cycle 2 by 0.5˚C in order to collect the melting curve data. The PCR reaction was put on hold by lowering the temperature to 4.0˚C. 28S-rRNA was used as housekeeping gene. To reduce variation, all experiments were determined in duplicate, and each experiment was repeated at least twice. cT Values of target genes were normalized to the cT Values of 28S-rRNA, whose expression levels have been shown to be constant under different experimental conditions (19-21). Differences in gene expression were calculated by $fold\ difference = 2^{(cT\ target\ gene\ R - cT\ target\ gene\ NR)}/2^{(cT\ housekeeping\ gene\ R - cT\ housekeeping\ gene\ NR)}$, NR, non-reversion; R, reversion.

Statistical analyses. Statistical significance for differences in cell morphology, cellular growth and gene expression was evaluated using the Student's *t*-test.

For analysis of microarray data, signal values were exported with the GeneChip operating software (GCOS, Affymetrix). Further analyses were performed with the software CorrXpression, which is described in detail elsewhere (22). For data normalization, the average of each experiment was placed in relation to the overall average calculated for all experiments. Over- and underexpression were defined whenever the expression value for each gene for each group (*e.g.* reversion phenotype) was higher or lower by at least a factor of two compared to each gene expression value for the other group (*e.g.* non-reversion phenotype). Due to the heterogeneity of human tumors, we attenuated the stringent ratio analysis conditions such that only 75% of the comparisons between reverted and non-reverted tumor specimens had to fulfill the criteria.

Using the Spearman rank correlation coefficient, the correlation between the Gene-Chip values and the expression data obtained by RT-PCR was statistically validated.

In all analyses, p-values≤ 0.05 were considered significant.

Results

Patients' characteristics. To analyze the impact of normal fibroblasts on growth and differentiation of breast carcinoma cells, PBCs were cultured as either monoculture or in co-culture with HMFs in a 3D-collagen-I matrix.

PBCs were isolated from tumors of a total of 13 patients with primary invasive breast cancer who had not received any neoadjuvant treatment. The histology of the tumor was validated by frozen-section analysis of tissue taken from the tumor before isolating the PBCs. Nine invasive ductal, three invasive lobular and one neuroendocrine carcinoma with diverse tumor stage, grade, HER2 status, and lymph node status were obtained. All tumors except one were estrogen- and/or progesterone receptor-positive (Table I).

Morphological analysis of 3D cell cultures. To explore whether PBCs are able to reverse their phenotype so as to resemble a normal polarized acinar architecture, PBCs were co-cultured with HMFs in 3D collagen-I gels and growth and morphology were compared to these for PBC monocultures.

Phenotypic reversion was defined by the formation of apico-basally polarized acinus-like structures of PBCs with

Table II. *Analysis of cell morphology and growth of primary breast cancer cells (PBCs) in 3D cultures. PBCs from 13 breast carcinomas were grown in 3D mono- and co-cultures with human mammary fibroblasts (HMFs). The percentage of multicellular structures with polarization of the cellular axis and lumen formation are shown. In each 3D culture, a minimum of 60 cell clusters was analyzed (inverted microscope; magnification: ×250). Growth of PBCs in 3D cultures is expressed as the total area of pancytokeratin-positive cells. Breast cancer samples 1-5 exhibited phenotypic reversion in 3D co-culture, breast cancer samples 6-13 did not show phenotypic reversion in 3D co-culture.*

Patient ID	Polarized acini (%) (SD)		*p*-Value	Total area* (SD)		*p*-Value	Phenotypic reversion
	Monoculture	Co-culture		Monoculture	Co-culture		
1	4.65 (0.55)	22.37 (0.92)	**<0.001**	0.11 (0.06)	0.17 (0.08)	**0.03**	+
2	13.68 (0.66)	24.78 (0.78)	**0.007**	0.23 (0.14)	0.41 (0.26)	**0.04**	+
3	1.75 (0.21)	12.63 (0.81)	**0.004**	0.13 (0.04)	0.11 (0.02)	0.22	+
4	15.13 (0.39)	25.81 (1.02)	**0.019**	0.18 (0.06)	0.26 (0.13)	0.07	+
5	5.34 (0.35)	15.15 (0.72)	**0.003**	0.28 (0.25)	0.38 (0.20)	0.28	+
6	4.62 (0.66)	4.48 (0.64)	0.930	0.10 (0.05)	0.16 (0.07)	**0.03**	–
7	13.83 (0.88)	14.19 (0.64)	0.968	0.30 (0.18)	0.47 (0.31)	0.12	–
8	15.63 (1.13)	20.97 (0.99)	0.353	0.16 (0.11)	0.14 (0.06)	0.55	–
9	23.44 (1.06)	24.29 (0.97)	0.884	0.21 (0.18)	0.18 (0.31)	0.70	–
10	18.33 (0.80)	21.88 (0.78)	0.434	0.18 (0.10)	0.16 (0.16)	0.80	–
11	7.69 (0.74)	11.11 (0.82)	0.845	0.16 (0.06)	0.21 (0.13)	0.27	–
12	14.29 (1.00)	19.15 (1.22)	0.434	0.09 (0.04)	0.13 (0.08)	0.18	–
13	20.63 (0.98)	22.97 (0.78)	0.622	0.09 (0.03)	0.1 (0.04)	0.57	–

+, Phenotypic reversion; –, no phenotypic reversion. *Quantitative analysis was performed after 9-10 days of culture and immunofluorescent staining for pancytokeratin. Twelve visual fields of each sample were analyzed with the Image J software, as described in Materials and Methods.

lumen formation reminiscent of a normal mammary gland. Using this approach, a reversion of the malignant phenotype was detected in five (38%) out of 13 PBC co-cultures with HMFs in comparison to the corresponding monocultures ($p \leq 0.02$) (Table II). In these cultures, the number of polarized acini in co-cultures was increased by about 2- to 7-fold. Within the reverted co-cultures, the carcinoma cells formed glandular structures, which were organized as a single layer of PBCs surrounding a hollow lumen. Interestingly, most of the acini were tightly-surrounded by HMFs (Figure 1 A-C; green arrows). Polarization of the cellular axis was identified by the expression of polarity markers. Establishment of apical polarity was shown by expression of a golgi protein (golgin-97) and tight junction protein zonula occludens protein-1 (ZO-1) at the apical membrane. PBCs also replicated the basal pole of the polarity axis as indicated by basally expressed β4-integrin, whereas β1-integrin assumed a basolateral location. Additionally, β-catenin was found to be expressed apicolaterally at the cell cell junctions (Figure 1 A).

The morphology of carcinoma cells in 3D monoculture was characterized by an unstructured organization of multicellular clusters as PBCs formed loose apolar colonies or grew as single cells. The expression of apical polarity markers golgin-97 and ZO-1 was reduced compared to reverted co-cultures and was randomly distributed. β1- and β4-integrin staining was dispersed membranous circumferentially, and β-catenin was diffusely expressed (Figure 1 A).

Vimentin expression is frequently found in carcinoma cells and serves as a marker for the epithelial mesenchymal transition (EMT) (23). In 3D monoculture, PBCs widely exhibited strong labeling for vimentin. In contrast, in reverted co-cultures carcinoma cells exhibited weak or lack of vimentin expression, implying that HMFs induce acinus formation, which is accompanied by mesenchymal epithelial transition (MET) (Figure 1 B).

Since the development and maintenance of baso-apical polarity is crucial for normal epithelial differentiation, we sought to explore whether reverted PBCs in co-culture display features of functional differentiation. Therefore, the mono- and co-culture of one of the reverted PBCs isolated were labeled for MAM-6, a glycoprotein that is transferred to the milk fat globule upon its secretion from acinar cells (24). A total of 71% of the acinar population in co-culture exhibited strong MAM-6 labeling within the lumina. In contrast, PBCs in monoculture failed to produce MAM-6 (Figure 1 C).

Additionally, assembly of a BM is a critical feature of normal mammary tissue function. Laminin-111, one of the major components of the BM, was found to be deposited basally around 32% of polarized acini in co-culture, whereas in 3D monoculture, laminin-111 was undetectable (Figure 1 C).

Eight co-cultures (62%) exhibited no significant difference in cell morphology compared to monocultures and were, therefore, classified as non-reverted. Although PBCs in these cultures exhibited varying degrees of polarized acinus

formation in both mono- and co-culture, no significant increase of acinar morphogenesis was observed in co-culture with HMFs (Table II). Morphological reversion of the malignant phenotype in 3D cell cultures was not associated with any histopathological characteristics of breast carcinomas (Table I).

Analysis of cell growth in 3D cell cultures. Mammary acinar morphogenesis is typically accompanied by epithelial growth arrest (2). On the other hand, fibroblasts have been shown to exhibit growth-stimulating and growth-suppressive effects on mammary epithelial cells (25). To investigate whether fibroblasts regulate growth of PBCs in 3D cultures, cell growth of PBCs in mono- and co-cultures was analyzed after 9 to 10 days of culture. Since the size of pancytokeratin-positive cell clusters correlates closely with the number of epithelial cell nuclei, the total cytokeratin-positive area can be used as a surrogate measure of cell numbers (26). Neither reverted nor non-reverted breast carcinomas showed a significant decrease of growth in co-cultures compared to monocultures. HMFs stimulated carcinoma cell growth in two reverted and one non-reverted 3D-culture (Table II). These data indicate that morphological reversion of breast carcinoma cells observed in 3D cultures is not linked to growth inhibition nor to stimulation by fibroblasts.

Gene expression analysis of tumors. Since phenotypic reversion was neither correlated with clinicopathological characteristics of the tumors nor with cellular growth in 3D co-cultures, we sought to identify molecular differences in the tumors from which PBCs were reverted and non-reverted using gene expression analysis.

A two-fold difference in expression between reverted and non-reverted co-cultures was defined as overexpression or underexpression. With this approach we identified 91 transcripts (84 genes) that were differentially expressed. Forty-two transcripts (38 genes) were found to be up-regulated in the revertible cases in comparison to the non-revertible cases. These included *ELF5* and *MAL* (Table III), which are known to play a role in the regulation of mammary gland development, differentiation of secretory epithelial cells and tumor suppression (28-32).

Forty-nine transcripts (46 genes) were down-regulated in the reverted cases in comparison to the non-reverted cases. Examples include *SQLE*, *ZMYND11*, and *MAP6* (Table IV), which have been shown to be involved in cancer progression and inhibition of differentiation (33-38).

Validation of the gene expression data. The Affymetrix data were validated by semi-quantitative real-time PCR. Three genes with up-regulated expression (*ELF5*, *MUCL1* and *PIP*) in reverted cases compared to the non-reverted cases and four genes with down-regulated expression (*MAP6, ZMYND11, LINGO1, SQLE*) were validated. For all but two genes (*SQLE, ZMYND11*) the results of the real-time PCR matched the Affymetrix data ($p \leq 0.01$). Even though for *SQLE* and *ZMYND11* there was no statistically significant correlation between the ΔCt values and the real-time PCR data, results were still consistent for these two techniques (Figure 2).

Discussion

The tissue microenvironment plays a critical role in the developmental regulation of normal and neoplastic cells. Here, we demonstrated that normal mammary fibroblasts are able to induce acinar morphogenesis and differentiation of PBCs in a 3D collagen-I cell culture model. In five out of 13 breast cancer samples, HMFs were able to revert the malignant phenotype of PBCs. In co-culture with HMFs, growth patterns of PBCs partly resembled those of normal mammary gland epithelium as PBCs formed regular, acinus-like spheroids, composed of a single layer of polarized cells surrounding a hollow lumen. Restoration of the complete baso-apical polarity axis was confirmed with established polarity markers. Furthermore, in reverted co-cultures, HMFs triggered functional differentiation of breast carcinoma cells, as indicated by secretion of the mammary tissue-specific glycoprotein MAM-6 and deposition of BM.

In contrast to co-cultures, PBCs in monoculture were characterized by disseminated and unstructured growth, forming loosely-disorganized apolar structures. Moreover, PBCs in monoculture exhibited expression of vimentin, which is frequently observed in breast cancer cells that have undergone EMT (23), whereas carcinoma cells in reverted co-cultures showed decreased or lack of vimentin expression. Therefore, it is tempting to speculate that normal fibroblasts are capable of inducing MET in breast carcinoma cells in a 3D environment.

In the normal mammary gland, acinar morphogenesis is accompanied by growth arrest of epithelial cells once the polarized colony is established (39). However, our results are consistent with these of Itoh *et al*. in that restoration of acinus formation triggered by stromal fibroblasts is not related to growth suppression (40).

Our findings that normal mammary fibroblasts are able to re-establish normal mammary gland morphology in PBC cultures support data from other investigators (41, 42). Following this idea, Lühr *et al*. examined whether the fibroblast type determines the response of epithelial cells in co-culture (15). Normal mammary epithelial cells were grown in co-cultures with primary cancer-associated fibroblasts (CAFs) or primary normal human mammary fibroblasts (NFs). Lühr *et al*. found that there was no difference in the growth behavior of epithelial cells in co-culture with either NF or CAF as both cell types were able to

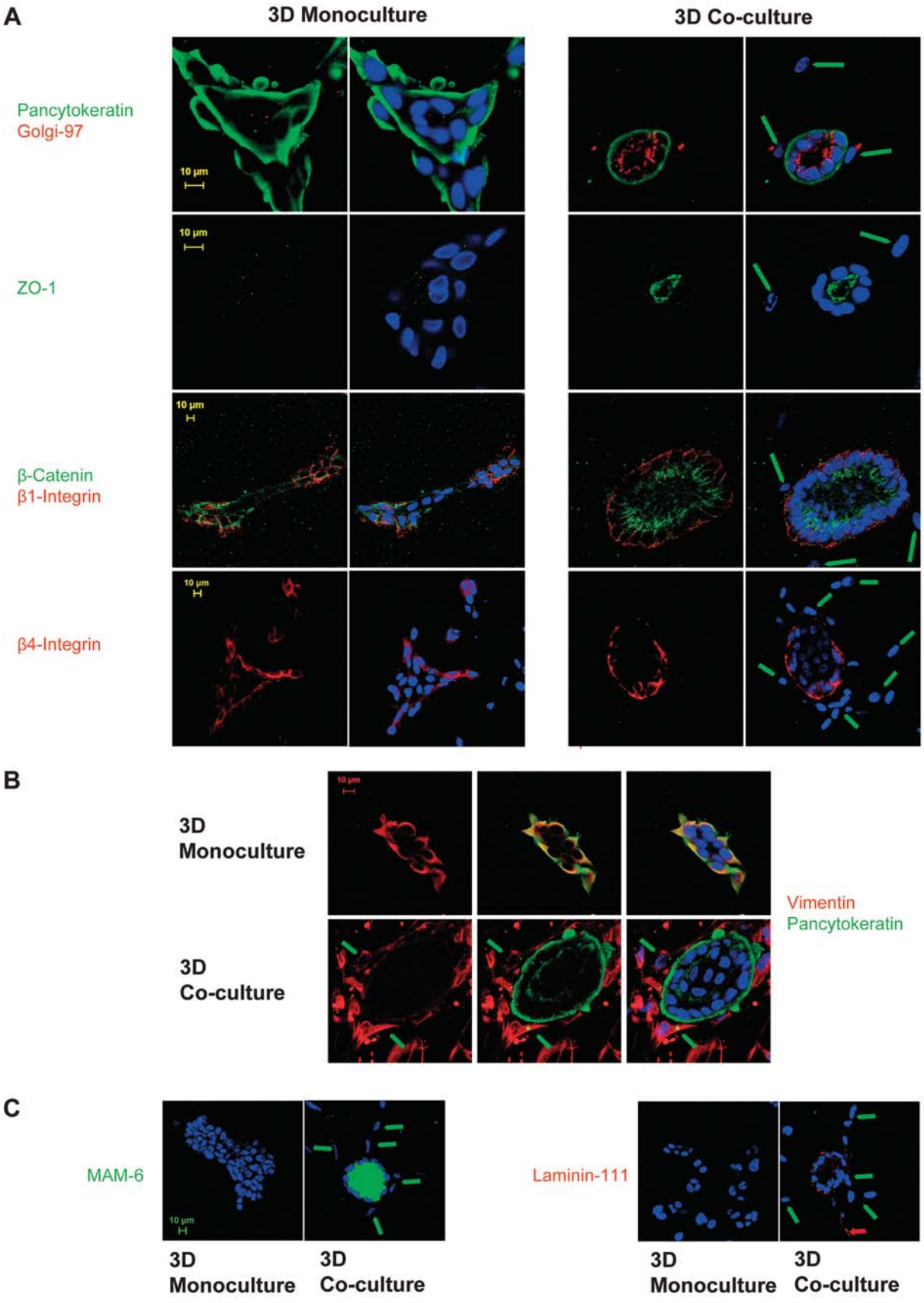
A
3D Monoculture
3D Co-culture
Pancytokeratin
Golgi-97
ZO-1
β-Catenin
β1-Integrin
β4-Integrin
10 μm
B
3D
Monoculture
3D
Co-culture
Vimentin
Pancytokeratin
C
MAM-6
Laminin-111
3D
Monoculture
3D
Co-culture
3D
Monoculture
3D
Co-culture

Table III. *Genes with up-regulated expression in reverted breast cancer cases compared with non-reverted breast cancer cases.*

Affymetrix probe set	Gene symbol	Fold change+	Gene name
226147_s_at	*PIGR*	18.62	Polymeric immunoglobulin receptor
1553602_at	*MUCL1*	7.71	Mucin-like-1
206439_at	*EPYC*	6.7	Epiphycan
206666_at	*GZMK*	6.09	Granzyme K (granzyme 3; tryptase II)
228233_at	*FREM1*	5.71	FRAS1-related extracellular matrix-1
209867_s_at	*LPHN3*	5.13	Latrophilin-3
205306_x_at	*KMO*	4.91	Kynurenine 3-monooxygenase (kynurenine 3-hydroxylase)
204205_at	*APOBEC3G*	4.77	Apolipoprotein B mRNA-editing, enzyme-catalytic, polypeptide-like 3G
206509_at	*PIP*	4.77	Prolactin-induced protein
206628_at	*SLC5A1*	4.62	Solute carrier family-5 (sodium/glucose cotransporter), member-1
240413_at	*PYHIN1*	4.56	Pyrin and HIN domain family, member-1
213802_at	*PRSS12*	4.28	Protease, serine, 12 (neurotrypsin, motopsin)
244203_at	*NA*	4.27	NA
204777_s_at	*MAL*	4.12	MAL, T-cell differentiation protein
210072_at	*CCL19*	4.06	Chemokine (C-C motif) ligand-19
1553204_at	*FLJ30313*	4.01	C20orf166 antisense RNA 1 (non-protein coding)
242670_at	*LGI4*	3.78	Leucine-rich repeat LGI family, member-4
214598_at	*CLDN8*	3.67	Claudin 8
231124_x_at	*LY9*	3.64	Lymphocyte antigen-9
230244_at	*C2orf82*	3.63	Chromosome 2 open reading frame 82
229629_at	*NA*	3.56	NA
204400_at	*EFS*	3.47	Embryonal FYN-associated substrate
205668_at	*LY75*	3.45	Lymphocyte antigen-75
1569225_a_at	*SCML4*	3.45	Sex comb on midleg-like-4 (Drosophila)
223075_s_at	*AIF1L*	3.41	Allograft inflammatory factor 1-like
220625_s_at	*ELF5*	3.35	E74-like factor 5 (ets domain transcription factor)
1557564_at	*NA*	3.19	NA
216050_at	*NA*	3.17	NA
1567224_at	*HMGA2*	3.15	High mobility group AT-hook-2
220646_s_at	*KLRF1*	3.11	Killer cell lectin-like receptor subfamily F, member-1
1555968_a_at	*NA*	3.0	NA
237201_at	*NA*	3.0	NA
1554250_s_at	*TRIM73*	2.93	Tripartite motif-containing-73
230110_at	*MCOLN2*	2.88	Mucolipin-2
1563473_at	*PPP1R16B*	2.85	Protein phosphatase 1 regulatory inhibitor subunit-16B isoform-1
242388_x_at	*TAGAP*	2.82	T-Cell activation GTPase activating protein
212239_at	*PIK3R1*	2.72	Phosphoinositide-3-kinase, regulatory subunit-1 (alpha)
1555392_at	*AY143171*	2.7	Testin-related protein TRG

NA, Not annotated. +Expression in reverted cases/non-reverted cases.

←

Figure 1. *Morphology of revertible breast carcinomas in 3D culture. A: Morphology of primary breast cancer cells (PBCs) in monoculture (upper panel) compared with cells in co-culture (lower panel) with normal human mammary fibroblasts (HMFs). Cells were labeled for apical [golgin-97 (red) and Zonula occludens protein-1 (ZO-1), (green)], basal [β4-integrin (red)], basolateral [β1-integrin (red)] and lateral [β-catenin (green)] polarity markers and epithelial [pancytoceratin (green)] markers. 3D Mono- and co-culture images in row 2 represent superimposed images with a nuclear counterstain [4',6-diamidino-2-phenylindole (DAPI) (blue)]. Green arrows: HMFs in co-culture. B: Reverted PBCs in 3D co-cultures down-regulate vimentin (red) expression compared to monocultures. Note that HMFs (green arrows) tightly surround the acinus formed by PBCs. Nuclear counterstain [DAPI (blue)]. The second column represents superimposed images of vimentin and pancytokeratin staining; the third column represents superimposed images of vimentin, pancytokeratin and DAPI staining. Note that the optical cross-section in 3D co-culture images does not exactly represent the middle of the acinus. C: Reverted PBCs 3D co-cultures exhibit functional differentiation. The 3D-culture of one reverted breast cancer case was further analyzed for functional differentiation. PBCs in 3D co-culture with HMFs form glandular structures with a hollow lumen, which is filled with secreted MAM-6 [left (green)]. The acinus is surrounded by a basement membrane containing laminin-111 [right (red)]. Green arrows: HMFs in co-culture. Red arrow: HMFs expressing laminin-111. Nuclear counterstain [DAPI (blue)].*

Table IV. *Genes with down-regulated expression in reverted breast cancer cases compared with non-reverted breast cancer cases.*

Affymetrix probe set	Gene symbol	Fold change	Gene name
216167_at	*LRRN2*	–11.23	Leucine rich repeat neuronal-2
226086_at	*SYT13*	–9.98	Synaptotagmin XIII
228010_at	*PPP2R2C*	–7.29	Protein phosphatase-2 (formerly 2A), regulatory subunit B, gamma isoform
223822_at	*SUSD4*	–5.63	Sushi domain containing-4
228943_at	*MAP6*	–5.62	Microtubule-associated protein-6
211273_s_at	*TBX1*	–5.2	T-Box-1
219425_at	*SULT4A1*	–4.7	Sulfotransferase family-4A, member-1
241352_at	*HEATR2*	–4.32	HEAT repeat containing-2
243105_at	*SUV420H1*	–4.27	Suppressor of variegation 4-20 homolog-1 (Drosophila)
206696_at	*GPR143*	–4.08	G-Protein-coupled receptor-143
234709_at	*CAPN13*	–3.95	Calpain-13
1557044_at	*NA*	–3.89	NA
205473_at	*ATP6V1B1*	–3.83	ATPase, H+ transporting, lysosomal 56/58kDa, V1 subunit-B1
1554159_a_at	*ZMYND11*	–3.76	Zinc finger, MYND-domain containing-11
1562226_at	*VWDE*	–3.61	Von Willebrand factor D and EGF domains
239739_at	*SNX24*	–3.58	Sorting nexin-24
227933_at	*LINGO1*	–3.55	Leucine-rich repeat and Ig domain containing-1
211205_x_at	*PIP5K1A*	–3.45	Phosphatidylinositol-4-phosphate 5-kinase, type-I, alpha
213562_s_at	*SQLE*	–3.45	Squalene epoxidase
1554887_at	*NA*	–3.44	NA
216855_s_at	*HNRNPU*	–3.36	Heterogeneous nuclear ribonucleoprotein U (scaffold attachment factor A)
230423_at	*NA*	–3.34	NA
243857_at	*MORF4L2*	–3.3	Mortality factor 4-like protein-2
216588_at	*RPL7*	–3.26	Ribosomal protein-L7
223232_s_at	*CGN*	–3.24	Cingulin
211427_s_at	*KCNJ13*	–3.11	Potassium inwardly-rectifying channel, subfamily J, member-13
232309_at	*NA*	–3.11	NA
235447_at	*TRUB1*	–3.1	TruB pseudouridine (psi) synthase homolog-1 (E. coli)
215281_x_at	*POGZ*	–2.92	Pogo transposable element with ZNF domain
1554575_a_at	*BPNT1*	–2.9	3'(2'), 5'-Bisphosphate nucleotidase-1
215249_at	*RPL35A*	–2.85	Ribosomal protein L35a
221926_s_at	*IL17RC*	–2.79	Interleukin-17 receptor C
233001_at	*SAMD10*	–2.72	Sterile alpha motif domain containing-10
223984_s_at	*NUPL1*	–2.71	Nucleoporin like-1
242091_at	*ZNF720*	–2.7	Zinc finger protein-720
206712_at	*GRTP1*	–2.66	Growth hormone-regulated TBC protein-1
211016_x_at	*HSPA4*	–2.66	Heat-shock 70 kDa protein-4
1563524_a_at	*ITPK1-AS1*	–2.65	ITPK1-AS1 ITPK1 antisense RNA 1 (non-protein coding)
243588_at	*FARP1*	–2.58	FERM, RhoGEF (ARHGEF) and pleckstrin domain protein-1 (chondrocyte-derived)
1565717_s_at	*FUS*	–2.54	Fused in sarcoma
243219_x_at	*MRPL50*	–2.51	Mitochondrial ribosomal protein L50
203441_s_at	*CDH2*	–2.49	Cadherin 2, type 1, N-cadherin (neuronal)
209872_s_at	*PKP3*	–2.47	Plakophilin-3
233248_at	*C1orf43*	–2.4	Chromosome 1 open reading frame 43
232466_at	*CUL4A*	–2.32	Cullin-4A
213472_at	*HNRNPH1*	–2.26	Heterogeneous nuclear ribonucleoprotein H

NA, Not annotated.

induce differentiation of mammary epithelial cells. Unpublished data of our working group demonstrate that T4-2 breast carcinoma cells undergo morphological reversion in 3D co-cultures with primary NFs and CAFs in a defined biomechanical environment, whereas Su *et al*. showed growth stimulation without differentiation of the breast cancer cell line T47D in co-cultures with CAFs (43). Taken together with our observations that we were not able to predict the ability of HMFs to induce reversion of the PBC phenotype by any parameter, one can assume that the restoration of differentiation is more influenced by specific epithelial cell characteristics rather than by the fibroblast

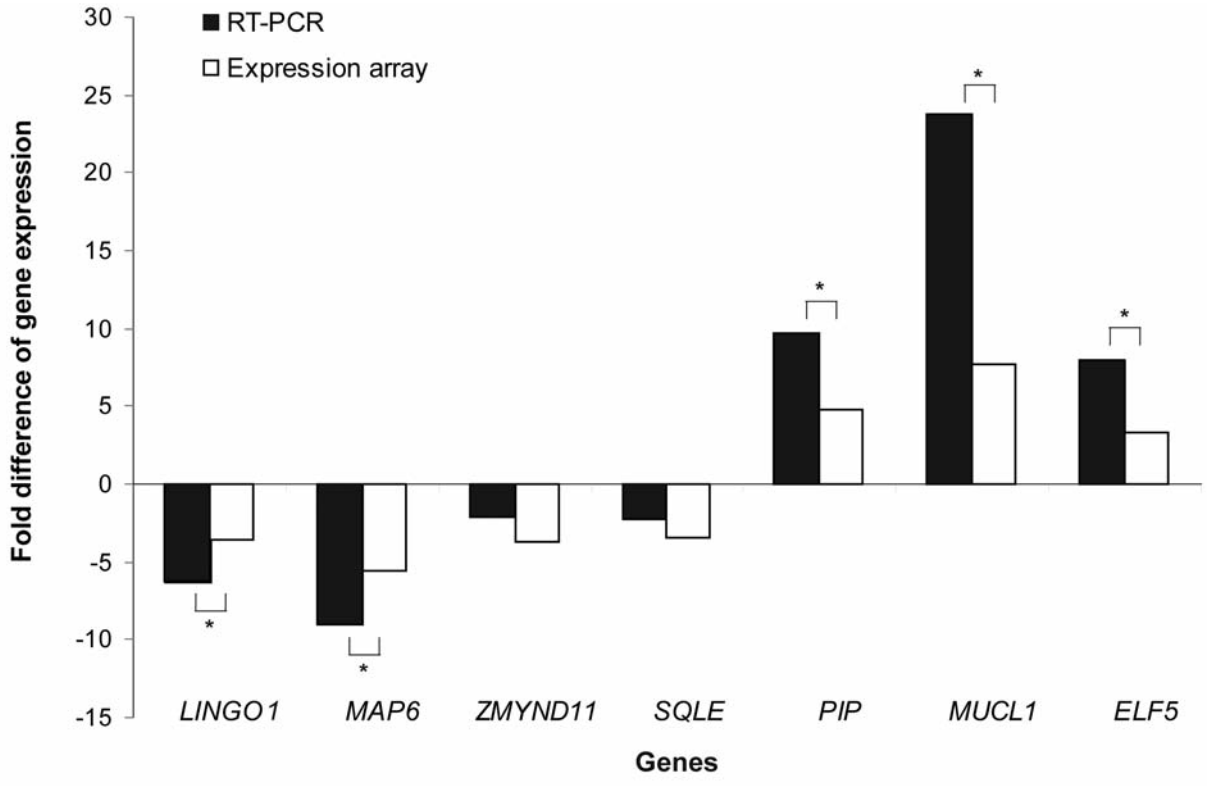

Figure 2. *Validation of mRNA levels of differentially regulated genes by RT-PCR. Seven differentially expressed genes were used to validate the array results. The mRNA levels of seven genes (three overexpressed in reverted cases, four underexpressed in reverted cases) were analyzed by quantitative RT–PCR in tumors from all 10 patients with breast cancer. The results are expressed as fold-difference between reversible and non-reversible cases. *Statistically significant positive correlation between RT-PCR data and expression values obtained by microarray analysis (p≤0.01).*

type. Evaluation of growth behavior of PBCs in 3D co-cultures with primary NFs and CAFs are the subject of our ongoing investigations.

3D Matrices composed of BM substitutes such as Matrigel® are frequently used to study differentiation of mammary epithelial cells (44, 45) as BM components, including laminin and nidogen-1, have been shown to be required for induction of polarization and differentiation of mammary epithelial cells (46, 47). Although in our experiments PBCs were cultured within a collagen-I matrix free of BM constituents, in 3D co-cultures a layer of laminin-111 was shown to surround the acinus formed by PBCs (Figure 1 C). Hence, we hypothesize that the production of BM components by HMFs and the subsequent establishment of a BM may account for the acinar morphogenesis of PBCs.

However, our experiments revealed that in eight out of 13 cases, normalizing the tumor microenvironment does not necessarily restore normal mammary gland architecture. This concept is underscored by the fact that we were not able to predict the ability of HMFs to induce phenotypic reversion by analyzing clinicopathological tumor characteristics, *e.g.* hormone receptor status, nodal status or grade. Furthermore, analysis of cell growth in mono- and co-cultures of reverted and non-reverted cases revealed that regulation of cell growth and phenotypic reversion are apparently uncoupled. These findings indicate that the reversion of the malignant phenotype is governed by differences in individual cases.

Since the formation of polarized epithelial tissues is known to be a dynamic process governed by reciprocal signaling events between the microenvironment and epithelial cells resulting in changes in gene expression (48), we sought for further explanations at the molecular level.

Gene expression analysis from five reverted and five non-reverted cases revealed different gene expression signatures between these two groups. Studying the list of differentially expressed genes, the function of two up-regulated (*MAL, ELF5*) and three down-regulated (*MAP6, ZMYND11, SQLE*) genes were informative to further elucidate the requirements for the reversion process.

MAL was found to be up-regulated in tumors which gave reverted co-cultures. This is consistent with its expression

being down-regulated in various epithelial tumor types (31, 49, 50) and hypermethylation of its gene promoter in breast cancer cell lines and primary breast cancer. Hence, up-regulation of *MAL* may indicate an increased tendency of PBCs to regain a non-malignant phenotype.

ELF5 is a major regulator of mammary gland development and differentiation (28, 51, 52) and is down-regulated in breast carcinomas, implying a suppressor function in breast cancer (53, 54). Therefore, overexpression of *ELF5* may reflect an increased ability of PBCs to differentiate in co-culture with HMFs.

In mantel cell lymphoma cell lines, *MAP6* amplification takes place during tumor progression (33). This observation may be consistent with our results, considering that *MAP6* was down-regulated in reverted cases.

Knockdown of *ZMYND11* in primary fibroblasts leads to cell-cycle arrest. Therefore, down-regulation of *ZMYND11* in reverted cases might be associated with response to apoptotic signals, particularly in view of the fact that *ZMYND11* is part of the p53-p21-CIP1 pathway (34).

Consistent with *SQLE* down-regulation in revertible cases, Helms *et al*. found *SQLE* to be up-regulated in breast carcinomas with gains of the chromosomes 7p and 8q and were able to identify a subset of patients with early-stage estrogen receptor-positive breast cancer with an increased risk of early metastasis (38). However, as expression levels of *ZMYND11* and *SQLE* determined by microarray analysis did not significantly correlate with measurements obtained by RT-PCR, these data need to be interpreted with caution.

Our findings demonstrate that the malignant phenotype of PBCs is not irreversible. Altering the cellular environment influences PBC differentiation patterns and likely their intracellular signaling pathways. We were able to revert the malignant phenotype of PBCs by culturing them with normal mammary fibroblasts in a 3D environment. Consistent with the inter-individually heterogeneous epithelial response to stromal reversion signals, we detected inter-individual differences at the molecular level. Although our results highlight a significant role of the tumor microenvironment in regulating morphogenesis and differentiation of tumors, further experiments are needed in order to decipher the reversion process and to identify all participating factors. Finally, normalization of the tumor microenvironment may be an innovative approach for future breast cancer therapy.

Acknowledgements

We thank Professor Dr. med. Dieter Kabelitz for enabling confocal analysis and Dr. rer. nat. Uwe Bertsch for their support with microscopy. We also thank Sigrid Hamann for her excellent technical assistance.

References

1 Polyak K and Kalluri R: The role of the microenvironment in mammary gland development and cancer. Cold Spring Harb Perspect Biol *2*: a003244, 2010.
2 Watson CJ and Khaled WT: Mammary development in the embryo and adult: a journey of morphogenesis and commitment. Development *135*: 995-1003, 2008.
3 Bissell MJ, Rizki A and Mian IS: Tissue architecture: the ultimate regulator of breast epithelial function. Current opinion in cell biology *15*: 753-762, 2003.
4 Wiseman BS and Werb Z: Stromal effects on mammary gland development and breast cancer. Science *296*: 1046-1049, 2002.
5 Mueller MM and Fusenig NE: Friends or foes – bipolar effects of the tumour stroma in cancer. Nat Rev Cancer *4*: 839-849, 2004.
6 Ronnov-Jessen L, Petersen OW and Bissell MJ: Cellular changes involved in conversion of normal to malignant breast: importance of the stromal reaction. Physiol Rev *76*: 69-125, 1996.
7 Matrisian LM, Cunha GR and Mohla S: Epithelial-stromal interactions and tumor progression: meeting summary and future directions. Cancer Res *61*: 3844-3846, 2001.
8 Bissell MJ and Radisky D: Putting tumours in context. Nat Rev Cancer *1*: 46-54, 2001.
9 Weaver VM, Petersen OW, Wang F, Larabell CA, Briand P, Damsky C and Bissell MJ: Reversion of the malignant phenotype of human breast cells in three-dimensional culture and in vivo by integrin blocking antibodies. J Cell Biol *137*: 231-245, 1997.
10 Wang F, Hansen RK, Radisky D, Yoneda T, Barcellos-Hoff MH, Petersen OW, Turley EA and Bissell MJ: Phenotypic reversion or death of cancer cells by altering signaling pathways in three-dimensional contexts. J Natl Cancer Inst *94*: 1494-1503, 2002.
11 Sandal T, Valyi-Nagy K, Spencer VA, Folberg R, Bissell MJ and Maniotis AJ: Epigenetic reversion of breast carcinoma phenotype is accompanied by changes in DNA sequestration as measured by AluI restriction enzyme. Am J Pathol *170*: 1739-1749, 2007.
12 Bissell MJ and Hines WC: Why don't we get more cancer? A proposed role of the microenvironment in restraining cancer progression. Nat Med *17*: 320-329, 2011.
13 Adriance MC, Inman JL, Petersen OW and Bissell MJ: Myoepithelial cells: good fences make good neighbors. Breast Cancer Res *7*: 190-197, 2005.
14 Kenny PA, Lee GY and Bissell MJ: Targeting the tumor microenvironment. Front Biosci *12*: 3468-3474, 2007.
15 Luehr I, Friedl A, Tholey A, Overath T, Kunze T, Hilpert F, Sebens S, Rösel F, Oberg HH, Maass N, Mundhenke C, Jonat W and Bauer M: Mammary fibroblasts regulate morphogenesis of normal and tumorigenic breast epithelial cells by mechanical and paracrine signals. 2012.
16 Jones JC: Reduction of contamination of epithelial cultures by fibroblasts. CSH Protoc 2008: pdb prot4478, 2008.
17 Kuperwasser C, Chavarria T, Wu M, Magrane G, Gray JW, Carey L, Richardson A and Weinberg RA: Reconstruction of functionally normal and malignant human breast tissues in mice. Proc Natl Acad Sci USA *101*: 4966-4971, 2004.
18 Su G, Blaine SA, Qiao D and Friedl A: Shedding of syndecan-1 by stromal fibroblasts stimulates human breast cancer cell proliferation *via* FGF2 activation. The Journal of biological chemistry *282*: 14906-14915, 2007.

19 Gong Y, Cui L and Minuk GY: Comparison of glyceraldehyde-3-phosphate dehydrogenase and 28s-ribosomal RNA gene expression in human hepatocellular carcinoma. Hepatology *23*: 734-737, 1996.
20 Wang EH, Truong LD, Mendoza L, Jung ES and Choi YJ: 28s-Ribosomal RNA is superior to glyceraldehyde-3-phosphate dehydrogenase as a RNA reference gene in p53-deficient mice with unilateral ureteral obstruction. Exp Mol Pathol *91*: 368-372, 2011.
21 Zhong H and Simons JW: Direct comparison of GAPDH, beta-actin, cyclophilin, and 28S rRNA as internal standards for quantifying RNA levels under hypoxia. Biochem Biophys Res Commun *259*: 523-526, 1999.
22 Klein A, Wessel R, Graessmann M, Jurgens M, Petersen I, Schmutzler R, Niederacher D, Arnold N, Meindl A, Scherneck S, Seitz S and Graessmann A: Comparison of gene expression data from human and mouse breast cancers: identification of a conserved breast tumor gene set. Int J Cancer *121*: 683-688, 2007.
23 Thiery JP: Epithelial mesenchymal transitions in tumour progression. Nat Rev Cancer *2*: 442-454, 2002.
24 Patton S, Gendler SJ and Spicer AP: The epithelial mucin, MUC1, of milk, mammary gland and other tissues. Biochim Biophys Acta *1241*: 407-423, 1995.
25 Kalluri R and Zeisberg M: Fibroblasts in cancer. Nat Rev Cancer *6*: 392-401, 2006.
26 Bauer M, Su G, Beebe DJ and Friedl A: 3D microchannel co-culture: method and biological validation. Integr Biol (Camb) *2*: 371-378, 2010.
27 Remmele W and Stegner HE: Recommendation for uniform definition of an immunoreactive score (IRS) for immunohistochemical estrogen receptor detection (ER-ICA) in breast cancer tissue. Pathologe *8*: 138-140, 1987 (in German).
28 Choi YS, Chakrabarti R, Escamilla-Hernandez R and Sinha S: Elf5 conditional knockout mice reveal its role as a master regulator in mammary alveolar development: Failure of Stat5 activation and functional differentiation in the absence of Elf5. Dev Biol *329*: 227-241, 2009.
29 Zhou J, Chehab R, Tkalcevic J, Naylor MJ, Harris J, Wilson TJ, Tsao S, Tellis I, Zavarsek S, Xu D, Lapinskas EJ, Visvader J, Lindeman GJ, Thomas R, Ormandy CJ, Hertzog PJ, Kola I and Pritchard MA: *Elf5* is essential for early embryogenesis and mammary gland development during pregnancy and lactation. Embo J *24*: 635-644, 2005.
30 Lee HJ, Hinshelwood RA, Bouras T, Gallego-Ortega D, Valdes-Mora F, Blazek K, Visvader JE, Clark SJ and Ormandy CJ: Lineage specific methylation of the *Elf5* promoter in mammary epithelial cells. Stem Cells *29*: 1611-1619, 2011.
31 Mimori K, Shiraishi T, Mashino K, Sonoda H, Yamashita K, Yoshinaga K, Masuda T, Utsunomiya T, Alonso MA, Inoue H and Mori M: *MAL* gene expression in esophageal cancer suppresses motility, invasion and tumorigenicity and enhances apoptosis through the Fas pathway. Oncogene *22*: 3463-3471, 2003.
32 Liebert M, Hubbel A, Chung M, Wedemeyer G, Lomax MI, Hegeman A, Yuan TY, Brozovich M, Wheelock MJ and Grossman HB: Expression of *MAL* is associated with urothelial differentiation *in vitro*: identification by differential display reverse-transcriptase polymerase chain reaction. Differentiation *61*: 177-185, 1997.
33 Vater I, Wagner F, Kreuz M, Berger H, Martin-Subero JI, Pott C, Martinez-Climent JA, Klapper W, Krause K, Dyer MJ, Gesk S, Harder L, Zamo A, Dreyling M, Hasenclever D, Arnold N and Siebert R: GeneChip analyses point to novel pathogenetic mechanisms in mantle cell lymphoma. Br J Haematol *144*: 317-331, 2009.
34 Zhang W, Chan HM, Gao Y, Poon R and Wu Z: BS69 is involved in cellular senescence through the p53-p21Cip1 pathway. EMBO Rep *8*: 952-958, 2007.
35 Hughes-Davies L, Huntsman D, Ruas M, Fuks F, Bye J, Chin SF, Milner J, Brown LA, Hsu F, Gilks B, Nielsen T, Schulzer M, Chia S, Ragaz J, Cahn A, Linger L, Ozdag H, Cattaneo E, Jordanova ES, Schuuring E, Yu DS, Venkitaraman A, Ponder B, Doherty A, Aparicio S, Bentley D, Theillet C, Ponting CP, Caldas C and Kouzarides T: EMSY links the BRCA2 pathway to sporadic breast and ovarian cancer. Cell *115*: 523-535, 2003.
36 Ekblad CM, Chavali GB, Basu BP, Freund SM, Veprintsev D, Hughes-Davies L, Kouzarides T, Doherty AJ and Itzhaki LS: Binding of EMSY to HP1beta: implications for recruitment of HP1beta and BS69. EMBO Rep *6*: 675-680, 2005.
37 Bennett LM, McAllister KA, Malphurs J, Ward T, Collins NK, Seely JC, Gowen LC, Koller BH, Davis BJ and Wiseman RW: Mice heterozygous for a *Brca1* or *Brca2* mutation display distinct mammary gland and ovarian phenotypes in response to diethylstilbestrol. Cancer Res *60*: 3461-3469, 2000.
38 Helms MW, Kemming D, Pospisil H, Vogt U, Buerger H, Korsching E, Liedtke C, Schlotter CM, Wang A, Chan SY and Brandt BH: Squalene epoxidase, located on chromosome 8q24.1, is up-regulated in 8q+ breast cancer and indicates poor clinical outcome in stage I and II disease. Br J Cancer *99*: 774-780, 2008.
39 Muschler J and Streuli CH: Cell-matrix interactions in mammary gland development and breast cancer. Cold Spring Harb Perspect Biol *2*: a003202, 2010.
40 Itoh M, Nelson CM, Myers CA and Bissell MJ: Rap1 integrates tissue polarity, lumen formation, and tumorigenic potential in human breast epithelial cells. Cancer Res *67*: 4759-4766, 2007.
41 DeCosse JJ, Gossens CL, Kuzma JF and Unsworth BR: Breast cancer: induction of differentiation by embryonic tissue. Science *181*: 1057-1058, 1973.
42 Krause S, Maffini MV, Soto AM and Sonnenschein C: The microenvironment determines the breast cancer cells' phenotype: organization of MCF7 cells in 3D cultures. BMC Cancer *10*: 263, 2010.
43 Su G, Sung KE, Beebe DJ and Friedl A: Functional screen of paracrine signals in breast carcinoma fibroblasts. PLoS One *7*: e46685, 2012.
44 Petersen OW, Ronnov-Jessen L, Howlett AR and Bissell MJ: Interaction with basement membrane serves to rapidly distinguish growth and differentiation pattern of normal and malignant human breast epithelial cells. Proc Natl Acad Sci USA *89*: 9064-9068, 1992.
45 Streuli CH, Bailey N and Bissell MJ: Control of mammary epithelial differentiation: basement membrane induces tissue-specific gene expression in the absence of cell-cell interaction and morphological polarity. J Cell Biol *115*: 1383-1395, 1991.
46 Pujuguet P, Simian M, Liaw J, Timpl R, Werb Z and Bissell MJ: Nidogen-1 regulates laminin-1-dependent mammary-specific gene expression. J Cell Sci *113(Pt 5)*: 849-858, 2000.

47 Streuli CH, Schmidhauser C, Bailey N, Yurchenco P, Skubitz AP, Roskelley C and Bissell MJ: Laminin mediates tissue-specific gene expression in mammary epithelia. J Cell Biol *129*: 591-603, 1995.

48 Bissell MJ, Hall HG and Parry G: How does the extracellular matrix direct gene expression? J Theor Biol *99*: 31-68, 1982.

49 Mori Y, Cai K, Cheng Y, Wang S, Paun B, Hamilton JP, Jin Z, Sato F, Berki AT, Kan T, Ito T, Mantzur C, Abraham JM and Meltzer SJ: A genome-wide search identifies epigenetic silencing of somatostatin, tachykinin-1, and 5 other genes in colon cancer. Gastroenterology *131*: 797-808, 2006.

50 Overmeer RM, Henken FE, Bierkens M, Wilting SM, Timmerman I, Meijer CJ, Snijders PJ and Steenbergen RD: Repression of MAL tumour suppressor activity by promoter methylation during cervical carcinogenesis. J Pathol *219*: 327-336, 2009.

51 Siegel PM and Muller WJ: Transcription factor regulatory networks in mammary epithelial development and tumorigenesis. Oncogene *29*: 2753-2759, 2010.

52 Harris J, Stanford PM, Sutherland K, Oakes SR, Naylor MJ, Robertson FG, Blazek KD, Kazlauskas M, Hilton HN, Wittlin S, Alexander WS, Lindeman GJ, Visvader JE and Ormandy CJ: Socs2 and Elf5 mediate prolactin-induced mammary gland development. Mol Endocrinol *20*: 1177-1187, 2006.

53 Ma XJ, Salunga R, Tuggle JT, Gaudet J, Enright E, McQuary P, Payette T, Pistone M, Stecker K, Zhang BM, Zhou YX, Varnholt H, Smith B, Gadd M, Chatfield E, Kessler J, Baer TM, Erlander MG and Sgroi DC: Gene expression profiles of human breast cancer progression. Proc Natl Acad Sci USA *100*: 5974-5979, 2003.

54 Sotgia F, Casimiro MC, Bonuccelli G, Liu M, Whitaker-Menezes D, Er O, Daumer KM, Mercier I, Witkiewicz AK, Minetti C, Capozza F, Gormley M, Quong AA, Rui H, Frank PG, Milliman JN, Knudsen ES, Zhou J, Wang C, Pestell RG and Lisanti MP: Loss of caveolin-3 induces a lactogenic microenvironment that is protective against mammary tumor formation. Am J Pathol *174*: 613-629, 2009.

Received January 24, 2013
Revised March 8, 2013
Accepted March 11, 2013